

# Exploring vector meson masses in nuclear collisions \*

B. K. Jain and Swapan Das  
Nuclear Physics Division, Bhabha Atomic Research Centre,  
Mumbai 400 085, India

Bijoy Kundu  
Institute of Physics, Sachivalaya Marg,  
Bhubaneswar 751 005, India

February 8, 2008

## Abstract

The formalism developed earlier by us for the propagation of a resonance in the nuclear medium in proton-nucleus collisions has been modified to the case of vector boson production in heavy-ion collisions. The first part of the talk describes this formalism. The formalism includes coherently the contribution to the observed di-lepton production from the decay of a vector boson inside as well as outside the nuclear medium. The calculated invariant rho mass distributions are presented for the  $\rho$ -meson production using optical potentials estimated within the VDM and the resonance model.

In the second part of the talk we write a formalism for coherent rho production in proton nucleus collisions and explore the sensitivity of the  $(p, p' \rho^0)$  reaction cross section to medium mass modification of the rho meson.

---

\*Talk delivered by B. K. Jain at National Seminar on Nuclear Physics, July 26-29, 1999, Institute of Physics, Bhubaneswar, India

# 1 Introduction

The modification of hadron masses in the nuclear medium is an issue of much interest currently [1]. Since in QCD the hadrons are excitations of the vacuum, it is natural that these excitations can get affected by the proximity of other hadrons. Experimentally the masses of unstable hadrons are explored by producing them in nuclear reactions and then measuring the invariant masses of their leptonic decay products [2]. The medium modification of the unstable hadron from these data is, normally, inferred by adding incoherently the decay of the hadron inside and outside the nuclear medium [3]. Recently formalisms have been developed by us [4] and Boreskov et al. [5] for the propagation of resonances produced in proton-nucleus collisions. These formalisms incorporate the interaction of the resonance with the nuclear medium. The invariant mass spectrum of the measured decay products in these formalisms is obtained by adding coherently the contribution of the resonance decay inside and outside the nuclear medium. The formalism of Jain et al. [4] also includes the interaction of the resonance decay products with the nuclear medium if the latter are hadrons. In the first part of the present talk we give the modification of our earlier formalism to heavy-ion collisions, and apply it to the propagation and decay of rho-meson. Our aim is to see how the medium modification of  $\rho$ -meson shows up in the di-lepton invariant mass distribution using a proper quantum mechanical description for the rho propagation in the nucleus. We do not compare our calculated results with the existing experimental data on rho-meson production in high energy heavy-ion collisions, because these data contain contribution from several other di-lepton processes than that considered in the present paper.

In the second part of the talk we write a formalism for coherent rho production in proton nucleus collisions and explore the sensitivity of the  $(p, p' \rho^0)$  reaction cross section to medium mass modification of the rho meson.

## 2 Heavy-ion collisions

### 2.1 Formalism

Let us suppose that two heavy nuclei, one the projectile  $A$  and another the target  $B$ , collide at high energies. We assume that one nucleon in the projectile and one in the target collide and a resonance  $R$  is produced at the collision point. This resonance then moves along the beam direction, which is taken as the  $z$ -axis, and decays at some subsequent point. Denoting by  $\mathbf{r}$  the relative coordinate between the target and the projectile, and by  $(\mathbf{r}_B, \mathbf{r}_A)$  the intrinsic coordinates of the target and projectile nucleons, respectively,

the resonance coordinate is written as,

$$\mathbf{r}_R = \mathbf{r}_A + \frac{B}{A+B} \mathbf{r}. \quad (1)$$

With this definition the ratio of the cross sections for the resonance production in AB and NN collisions, for an inclusive situation where the state of the (A+B) system is not identified, can be written as,

$$\frac{\Delta\sigma_R^{AB}}{\Delta\sigma_R^{NN}} = [K.F.] \int d\mathbf{b} \int dz \int d\mathbf{r}_A \rho_A(\mathbf{r}_A) \rho_B(\mathbf{r} + \mathbf{r}_A) |G(\mathbf{r}_R; \mathbf{k}_R, \mu)|^2, \quad (2)$$

where  $\rho_x$  are the nuclear densities. [K.F.] is the relevant kinematical factor. The function  $G(\mathbf{r}_R; \mathbf{k}_R, \mu)$  physically gives the probability amplitude for finding the decay products of the resonance in the detector with the total momentum  $\mathbf{k}_R$  and the invariant mass  $\mu$ , if the resonance is produced at a point  $\mathbf{r}_R$  in the nucleus (for details see Ref. [4, 5]). In terms of the resonance propagator  $G(\mathbf{r}'_R, \mathbf{r}_R)$ , the function  $G(\mathbf{r}_R; \mathbf{k}_R, \mu)$  is defined as

$$G(\mathbf{r}_R; \mathbf{k}_R, \mu) = \int d\mathbf{r}'_R \exp(-i\mathbf{k}_R \cdot \mathbf{r}'_R) G(\mathbf{r}'_R, \mathbf{r}_R), \quad (3)$$

where  $G(\mathbf{r}'_R, \mathbf{r}_R)$  satisfies

$$[\nabla^2 + E^2 - m_R^2 + i\Gamma_R m_R - \Pi_R] G(\mathbf{r}'_R, \mathbf{r}_R) = \delta(\mathbf{r}'_R - \mathbf{r}_R). \quad (4)$$

Here  $\Pi_R$  is the self energy of the resonance in the medium and  $\Gamma_R$  is its free space decay width.

In the eikonal approximation we can write,

$$G(\mathbf{r}_R; \mathbf{k}_R, \mu) = \exp(-i\mathbf{k}_R \cdot \mathbf{r}_R) \phi_R(\mathbf{r}_R; \mathbf{k}_R, \mu), \quad (5)$$

where  $\phi_R$  is a slowly varying modulating function. With this, and using the Eqs. (3,4),  $\phi_R$  approximately works out to

$$\begin{aligned} \phi(\mathbf{r}_R; \mathbf{k}_R, \mu) &= \frac{1}{2ik_R} \int dz'_R \exp\left[\frac{1}{2ik_R}(\mu^2 - m_R^2 + i\Gamma_R m_R)(z_R - z'_R)\right] \\ &\times \exp\left[\frac{-i}{v_R} \int_{z_R}^{z'_R} V_R(b_R, z'') dz''\right]. \end{aligned} \quad (6)$$

Here we have written

$$\Pi_R = 2E_R V_R, \quad (7)$$

where  $V_R$  is the optical potential of the resonance, R, in the nuclear medium. In general, it is complex. Its real part, as we shall see later, is related to the mass shift of the resonance and the imaginary part gives the collision broadening of the resonance in the medium.

For a nucleus with a sharp surface, function  $\phi(\mathbf{r}_R; \mathbf{k}_R, \mu)$  splits into a sum of two terms, one corresponding to the decay of the resonance inside the nucleus and another to the decay outside the nucleus, i.e.

$$\phi(\mathbf{r}_R; \mathbf{k}_R, \mu) = \phi_{in}(\mathbf{r}_R) + \phi_{out}(\mathbf{r}_R) \quad (8)$$

with

$$\phi_{in}(\mathbf{r}_R) = \frac{1}{2ik_R} \int_{z_R}^{\sqrt{(R^2 - b^2)}} dz'_R \phi_R(\mathbf{b}_R; z_R, z'_R), \quad (9)$$

and

$$\phi_{out}(\mathbf{r}_R) = \frac{1}{2ik_R} \int_{\sqrt{(R^2 - b^2)}}^{\infty} dz'_R \phi_R(\mathbf{b}_R; z_R, z'_R). \quad (10)$$

Here

$$\begin{aligned} \phi_R(\mathbf{b}_R; z_R, z'_R) &= \exp\left[\frac{1}{2ik_R}(\mu^2 - m_R^2 + i\Gamma_R m_R)(z_R - z'_R)\right] \\ &\times \exp\left[\frac{-i}{v_R} \int_{z_R}^{z'_R} V_R(b_R, z''_R) dz''_R\right]. \end{aligned} \quad (11)$$

After a little bit of manipulations, the final expressions for  $\phi_{in}$  and  $\phi_{out}$  work out to ,

$$\phi_{in}(\mathbf{r}_R; k_R, \mu) = \frac{G_0^*}{2m_R} [1 - \exp(\frac{i}{v_R G_0^*} [L(b_R) - z_R])], \quad (12)$$

$$\phi_{out}(\mathbf{r}_R; k_R, \mu) = \frac{G_0}{2m_R} [\exp(\frac{i}{v_R G_0^*} [L(b_R) - z_R])], \quad (13)$$

where  $v_R$  is the speed of the resonance and  $L(= \sqrt{(R^2 - b_R^2)})$  is the length from the production point to the surface of the nucleus.  $G_0$  and  $G_0^*$  in Eqs. (12) and (13) are the free and the in-medium resonance propagators. Their forms are

$$G_0 = \frac{2m_R}{\mu^2 - m_R^2 + i\Gamma_R m_R}, \quad (14)$$

$$G_0^* = \frac{2m_R}{\mu^2 - m_R^{*2} + i\Gamma_R^* m_R}, \quad (15)$$

with

$$m_R^* \approx m_R + \frac{E_R}{m_R} U_R. \quad (16)$$

Table 1: Rho-meson optical potentials following Ref. [7] for  $\mu=770$  MeV.

$v/c$	U(MeV)	W(MeV)
0.04	-20.4	-40.8
0.6	37.9	-50.6
0.9	25.8	-54.7

$$\Gamma_R^* = \Gamma_R + \frac{E_R}{m_R} |2W_R|. \quad (17)$$

It may be mentioned that, for a nucleus with no sharp surface approximation the expression given in Eq. (6) can be used directly to evaluate the function  $\phi(\mathbf{r}_R; \mathbf{k}_R, \mu)$ .

In the above we have written,

$$V_R = U_R + iW_R. \quad (18)$$

These potentials, as given in Eqs. (16,17) give a measure of the mass and width modification of the resonance in the nuclear medium. Their values are an open question and a subject of much research internationally. In one approach they can be treated as completely unknown quantities and data on appropriate experiments can be used to extract their values. This exercise would be of use if the theoretical formalism used describes the reaction dynamics correctly and the data do not have much uncertainty. Alternatively, they can be estimated in a particular model and the ensuing values can be used to make an estimate of the cross section for the rho production. In literature, various efforts [6, 7] have been made to estimate  $V_R$  using the high energy ansatz, i.e.

$$U_R = -\alpha \left[ \frac{1}{2} v_R \sigma_T^{RN} \rho_0 \right] \quad (19)$$

and

$$W_R = -\left[ \frac{1}{2} v_R \sigma_T^{RN} \rho_0 \right], \quad (20)$$

where  $\alpha$  is the ratio of the real to the imaginary part of the elementary RN scattering amplitude and  $\sigma_T^{RN}$  is the total cross section for it.  $\rho_0$  is the typical nuclear density. A detailed calculation for the rho-meson has been done on these lines by Kondrayuk et al. [7] which give these potentials as a function of momentum. They use VDM at high energies and resonance model at low energies to generate the  $\rho$ N scattering parameters. We have used these values for our calculations in the present paper. Some representative values of the self energies required in our calculations are given in Table 1.

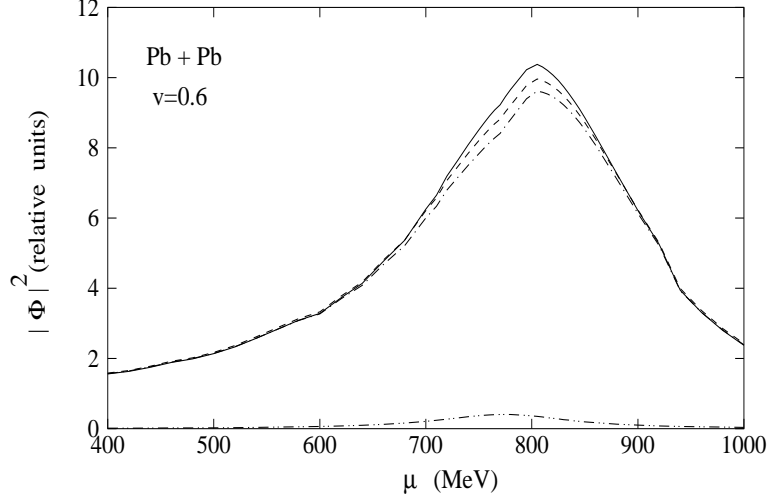


Figure 1: The invariant mass spectra of the  $\rho$  meson produced in Pb+Pb collisions. The solid curve is obtained after adding the inside and the outside decay coherently, while the dashed curve is obtained by adding the same incoherently. The dash-dot curve is the inside decay contribution and the dash-dot-dot curve is the outside decay contribution separately. The resonance speed is  $0.6c$ .

## 2.2 Results and Discussion

Examining Eqs. (9-11)  $\phi(\mathbf{r}_R; \mathbf{k}_R, \mu)$  in above we find that the cross sections for the decay of the resonance in the nucleus depends upon the length of the nuclear medium, the speed ( $v_R$ ), free decay width and self energy of the resonance. To represent the effect of all these quantities, we present results for the decay of the rho-meson for different values of  $v_R$  and for two sets of nuclear systems, viz.  $Pb + Pb$  and  $S + Au$ . The free width of the rho-meson is taken equal to 150 MeV. The optical potentials, which we need at several  $\rho$  momenta, are taken, as mentioned above, from Kondratyuk et al. [7]. Nuclear densities are taken from Ref. [8].

Denoting the ratio  $\frac{1}{[K.F.]} \frac{\Delta\sigma_R^{AB}}{\Delta\sigma_R^{NN}}$  in Eq. (2) as  $|\Phi|^2$ , we plot  $|\Phi|^2$  as a function of the invariant mass,  $\mu$ , of the decay products of the  $\rho$  meson. Figures 1-4 show the invariant mass spectra of the  $\rho$  meson in  $Pb + Pb$  and  $S + Au$  collisions at rho velocities of  $0.6c$  and  $0.9c$ . Here  $c$  is the speed of light. The solid curve in all the figures gives the coherently summed cross-section from the decay of  $\rho$ -meson inside and outside the nuclear medium. The dashed curve gives the same added incoherently. The individual contributions corresponding to the inside and the outside decay are given by the dash-dot and dash-dot-dot curves respectively. We observe two things. One, the coherent and the incoherent cross-sections are different and second, this difference increases with the increase in the rho-meson speed. At  $0.6c$  speed, while the coherent and incoherent curves

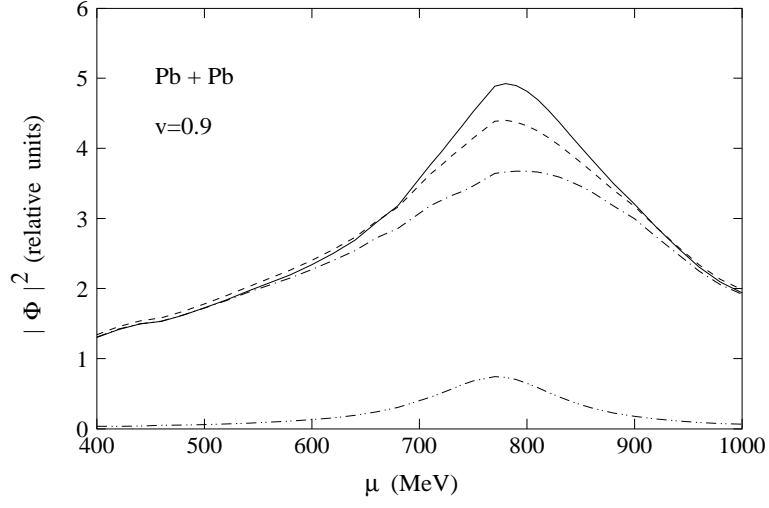


Figure 2: All curves have same meaning as in Fig. 1. The resonance speed is  $0.9c$ .

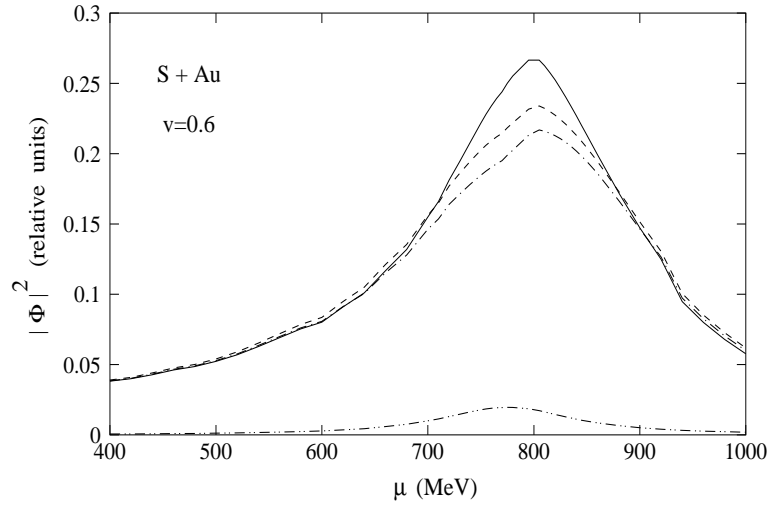


Figure 3: All curves have same meaning as in Fig. 2. The colliding nuclear system is S+Au and the resonance speed is  $0.6c$ .

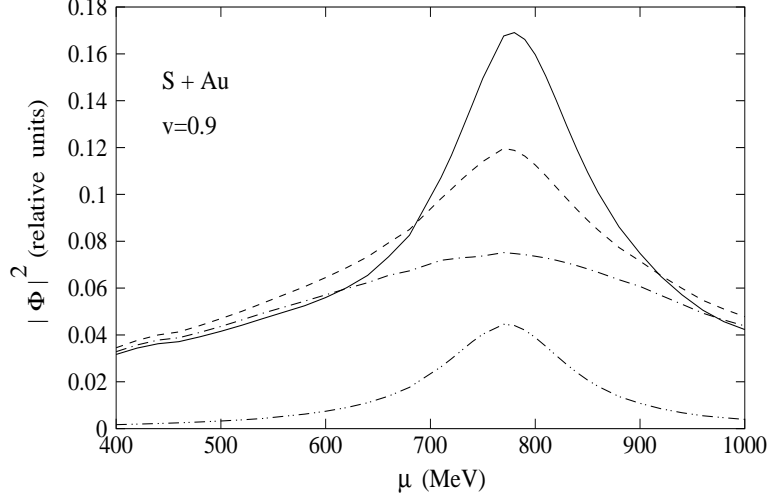


Figure 4: Same as in Fig. 3. The resonance speed is  $0.9c$ .

differ only in the peak cross sections, at  $0.9c$  speed their shape and peak cross sections both are different. We also observe that the difference is larger for the smaller system like S on Au. If we compare the mass shift seen in our calculations (Figs. 1-4) with those indicated in the high energy heavy ion collisions, our shifts are small and are in the opposite direction. To explore as what kind of optical potentials would produce a shift as large as those indicated experimentally we calculated  $|\Phi|^2$  for Pb+Pb at  $0.9c$  for three arbitrarily chosen values of  $U_R$ , viz.  $-40$ ,  $-80$  and  $-120$  MeV. These results are shown in Fig. 5. We find that only with  $-120$  MeV value the distribution starts having features resembling those indicated in heavy-ion experiments. But this value, compared with the value around  $+25$  MeV coming from the high energy ansatz of Kondratyuk et al. (see Table 1) is very large and is of opposite sign.

### 3 Proton-nucleus collisions

The cross section for a coherent rho production reaction,  $(p, p' \rho^0)$ , is given by

$$d\sigma = [PS] S(m^2) < |T_{coh}|^2 >, \quad (21)$$

where the phase-space factor,  $[PS]$ , is written as

$$[PS] = \frac{\pi m_p^2 m_A}{(2\pi)^6} \frac{k_{p'} k_\rho^2}{k_p [k_\rho (E_i - E_{p'}) - (\mathbf{k}_p - \mathbf{k}_{p'}) \cdot \hat{k}_\rho E_\rho]} dm^2 dE_{p'} d\Omega_{p'} d\Omega_\rho. \quad (22)$$

$S(m^2)$  is the free space rho mass distribution function, which is given by

$$S(m^2) = \frac{1}{\pi} \frac{m_\rho \Gamma_\rho}{[(m^2 - m_\rho^2)^2 + m_\rho^2 \Gamma_\rho^2]}, \quad (23)$$



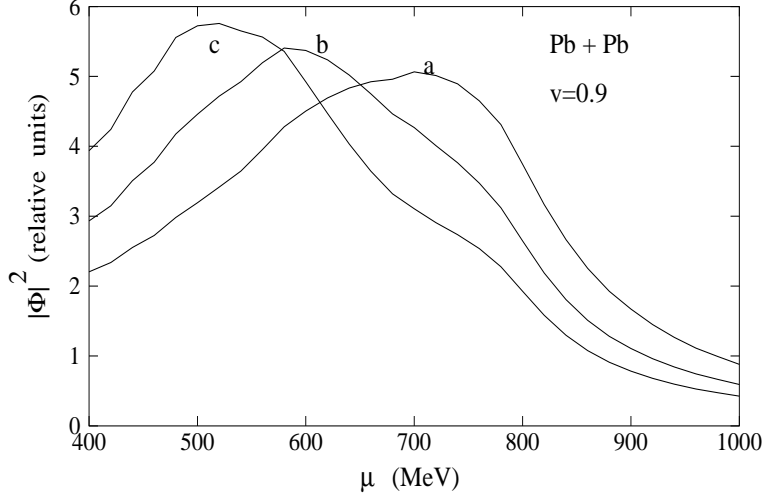


Figure 5: Sensitivity of the cross-section to the amount of mass modification of the rho-meson. The calculations are presented for Pb+Pb system at 0.9c rho-meson speed. Curves 'a', 'b' and 'c' are for  $U_R$  equal to -40, -80 and -120 respectively. The imaginary part of the optical potentials is the same as used in Fig. 2.

with  $m_\rho = 770$  MeV and  $\Gamma_\rho = 150$  MeV.

The T-matrix,  $T_{coh}$ , is given by

$$T_{coh} = (\chi_{\mathbf{k}_{p'}}^{(-)*}, \Psi_{\mathbf{k}_\rho}^{(-)*} < p', \rho^0 | \mathcal{L}_{\rho NN} | p > \chi_{\mathbf{k}_p}^{(+)}), \quad (24)$$

where  $\chi$ 's denote the distorted waves for the incoming and outgoing protons. However, in the energy region of interest for rho production the distortion effects are mainly absorptive. Therefore, the proton distorted waves in above can be replaced by plane waves for the present purpose.

$\Psi_{\mathbf{k}_\rho}^{(-)*}$  is the  $\rho$ -meson scattering wave function with asymptotic momentum  $\mathbf{k}_\rho$ . It has the form

$$\Psi_{\mathbf{k}_\rho}^{(-)*} = e^{-i\mathbf{k}_\rho \cdot \mathbf{r}} + \Psi_{scat.}^* \quad (25)$$

In the absence of any dispersive nuclear distortion of  $p$  and  $p'$ , the first term in this equation does not contribute to  $T_{coh}$  because  $\mathbf{k}_\rho \neq \mathbf{k}_p - \mathbf{k}_{p'}$ . This in other words means that the rho meson produced at the proton vertex is off-shell. It can not be seen in the detector without incorporating the medium effects on it.  $\Psi_{scat.}$  is the part of the wave function which include these effects. If we associate a self energy  $\Pi (= 2\omega V$ , where  $V$  is the corresponding optical potential) with the  $\rho$ -meson,  $\Psi_{scat.}$  is given by

$$\Psi_{scat.}^* = \chi_{\mathbf{k}_\rho}^{(-)*} V G_\rho(t), \quad (26)$$

where  $\chi_{\mathbf{k}_\rho}^{(-)*}$  is the scattering solution of the potential  $V$ .  $G_\rho(t)$  is the  $\rho$ -meson propagator,

Table 2: Optical potentials for certain values of the  $\rho$  momentum.

$k_\rho$ (MeV/c)	30	50	75	100	500
U (MeV)	-20.75	-9.27	-0.37	5.90	33.49
W (MeV)	-26.51	-30.46	-34.79	-42.09	-46.73

and is given by

$$G_\rho(t) = -\frac{2\omega}{m_\rho^2 - t - i\omega\Gamma_\rho}. \quad (27)$$

$t(= \omega^2 - \mathbf{q}^2)$  is the four-momentum transfer squared to  $\rho$ -meson at the production vertex.

For the  $\rho$  production Lagrangian in Eq. (24) we have taken

$$\mathcal{L}_{\rho NN} = \frac{fF(t)}{m_\rho} N^\dagger (\sigma \mathbf{x} \mathbf{q}) \tau N \cdot \rho, \quad (28)$$

with  $\rho$ NN coupling constant,  $f$ , equal to 7.81, and the off-shell extrapolation form factor as

$$F(t) = \frac{\Lambda^2 - m_\rho^2}{\Lambda^2 - t}, \quad (29)$$

with  $\Lambda = 2$  GeV/c.

With the above formalism we calculate the  $\rho$  production cross section for the  $^{12}\text{C}$  target nucleus. The only quantity required for the calculation is the description of the optical potential,  $V$ , of the  $\rho$ -meson. The values of the optical potential are fixed using the same prescription as given earlier for the heavy ion reactions. Some representative values required by us are given in Table 2. The radial shape of the optical potential is approximated by the radial density distribution of the  $^{12}\text{C}$  nucleus.

In Fig. 6 we plot the calculated outgoing proton energy spectrum for  $p'$  going very near to the forward direction against the energy transfer  $\omega(=T_p - T_{p'})$ . This energy transfer and the corresponding momentum transfer  $\mathbf{q}(=\mathbf{k}_p - \mathbf{k}_{p'})$  are shared between the rho-meson and the recoiling nucleus through the interaction of the rho-meson with the target nucleus. The beam energy is taken equal to 1.5 GeV. We see in the figure that the calculated distribution has a broad peak. The peak cross section is around  $0.34 \mu\text{b}/\text{MeV}$ .

In Fig. 7 we show the angular distribution of the above rho-mesons at the peak position in Fig 6. It is observed that most of the rho-meson flux gets emitted in the forward direction only. Very little is seen beyond  $15^\circ$  or so.

Above results are given for a certain choice of the  $\rho$ -meson optical potential. However, they would be sensitive to the change in this potential. In Fig. 8 we have investigated this sensitivity. The optical potential for this purpose has been taken purely real, and

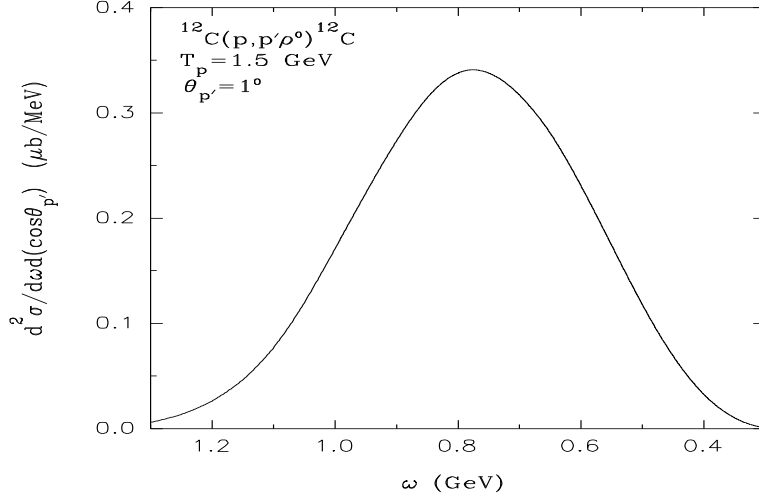


Figure 6: Calculated energy spectrum for the outgoing proton near forward angle as a function of the energy transfer  $\omega (= T_p - T_{p'})$  for  $^{12}\text{C}(p, p'\rho^0)^{12}\text{C}$  reaction integrated over all emission angles of the  $\rho^0$ -meson. The beam energy is 1.5 GeV and the optical potentials are given in Eqs. (19) and (20).

different values for it are fixed through different mass-shifts of the  $\rho$ -meson in the medium using the relation given in Eq. (16). In Fig. 8 we show the calculated proton energy spectrum for  $\Delta m (= m - m^*)$  taken equal to 50, 100 and 150 MeV. On x-axis, instead of  $\omega$ , we have  $\frac{\omega}{\Delta m}$ . This is done because the essential parameter determining the dynamics of the rho-meson in the potential is likely to be the rho energy relative to the depth of the potential. We observe that

1. the magnitude of the cross sections increases with the increase in the strength of the potential.
2. In addition to the broad peak, we see a sharp peak in the small energy region of the rho-meson. The position of this peak on the  $\frac{\omega}{\Delta m}$  scale is around 3.7 for  $\Delta m = 100$  and 150 MeV. For  $\Delta m = 50$  MeV, this peak is not seen in the results because by then the cross section becomes too small.

On examining the phase-shifts of the scattered wave function of rho-meson in the potential, we find that the sharp peak is like a shape elastic resonance seen in the elastic scattering experiments.

Of course, when the  $\rho$ -potential is made complex, as is in Fig. 6 the sharp peak disappears.

To summarize, we find that in proton scattering on nuclei a measurable cross section exists for  $\rho$  meson production due to coherent effect of the target nucleus. The actual

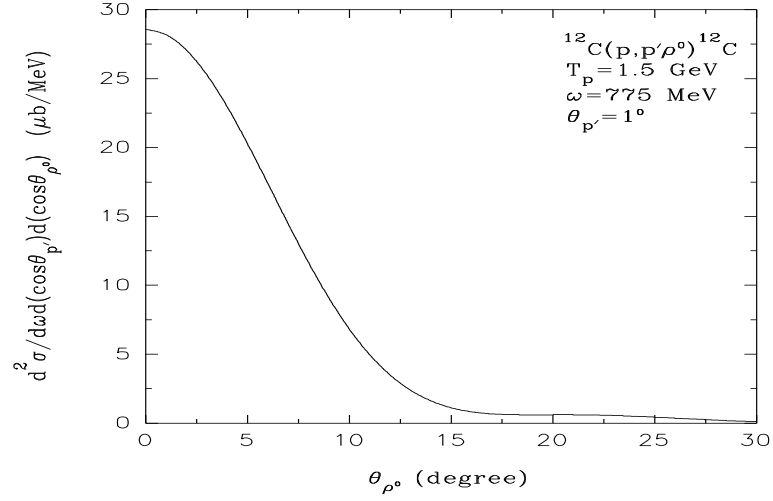


Figure 7: Calculated angular distribution of the  $\rho^0$ -meson for the energy transfer ( $\omega$ ) at the peak in Fig. 6.

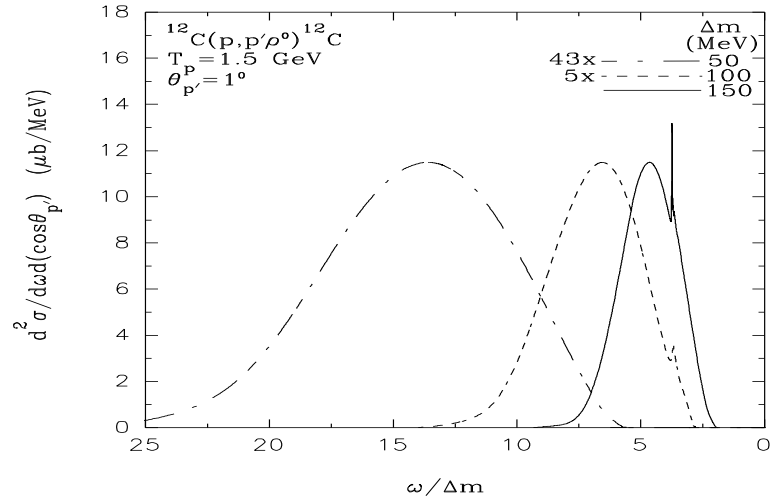


Figure 8: Calculated energy spectrum for the outgoing proton near forward direction as a function of the energy transfer  $\omega$  in the units of  $\rho^0$ -meson mass-shift,  $\Delta m$ , at 1.5 GeV beam energy for different values of the mass-shift.

magnitude of the cross section depends sensitively on the strength of the  $\rho$ -meson optical potential, which is related to the rho-mass modification in the nuclear medium. The cross section increases with the increase in the potential strength. The angular distribution of the emitted rho-meson is such that most of them go in a forward cone of about  $15^\circ$ . For a purely real potential a sharp peak appears in the proton energy spectrum in the region of the small rho-meson energy.

The authors acknowledge many useful discussions they had with Shashi Phatak and A. B. Santra, and thank them for the same.

## References

- [1] G. E. Brown and M. Rho, Phys. Rev. Lett. 66 (1991) 2720; T. Hatsuda and S. H. Lee, Phys. Rev. C 46 (1992) R34; J. D. Walecka, Ann. Phys. (N.Y.) 83 (1974) 491; B. D. Serot and J. D. Walecka, Adv. Nucl. Phys. 16 (1986) 1; Int. J. Mod. Phys. E 6 (1997) 515; H. Shiomi and T. Hatsuda, Phys. Lett. B 334 (1994) 281; M. Herrmann, B. L. Friman and W. Nörenberg, Nucl. Phys. A 560 (1993) 411; M. Asakawa and C. M. Ko, Phys. Rev. C 48 (1993) R526; M. Asakawa, C. M. Ko, P. Lévai and X. J. Qiu, Phys. Rev. C 46 (1992) R1159; K. Saito, K. Tsushima and A. W. Thomas, Phys. Rev. C 56 (1997) 566.
- [2] A. Drees, Nucl. Phys. A 610 (1996) 536c;  
CERES Collaboration, Th. Ullrich, Nucl. Phys. A 610 (1996) 317c;  
HELIOS-3 Collaboration, M. Maser, Nucl. Phys. A 590 (1995) 93c;  
NA50 Collaboration, E. Scapparini, Nucl. Phys. A 610 (1996) 331c.
- [3] R. S. Bhalerao and S. K. Gupta, Mod. Phys. Lett. A 12 (1997) 127.
- [4] B. K. Jain and B. Kundu Phys. Rev. C 53 (1996) 1917.
- [5] K. G. Boreskov et al., Nucl. Phys. A 619 (1997) 295.
- [6] B. Friman, Nucl. Phys. A 610 (1996) 358c; V. L. Eletsky and B. L. Ioffe, Phys. Rev. Lett. 78 (1997) 1010; V. L. Eletsky, B. L. Ioffe and J. I. Kapusta, Eur. Phys. J. A 3 (1998) 381.
- [7] L. A. Kondratyuk, A. Sibirtsev, W. Cassing, Ye. S. Golubeva and M. Effenberger, Phys. Rev. C 58 (1998) 1078.
- [8] H. De Vries and C. W. De Jager, Atomic and Nuclear data tables 36 (1987) 495.